Proc. Natl. Acad. Sci. USA
Vol. 93, pp. 9565–9570, September 1996
Cell Biology

Defective propagation of signals generated by sympathetic nerve stimulation in the liver of connexin32-deficient mice

[gap junctions/glucose release/metabolic cooperation/Charcot–Marie–Tooth disease (CMTX)]

ERIC NELLES*†, CHRISTOPH BÜTZLER*†, DIRK JUNG*, ACHIM TEMME*, HEINZ-DIETER GABRIEL*, URSULA DAHL*, OTTO TRAUB*, FRANK STÜMPEL‡, KURT JUNGERMANN‡, JÜRGEN ZIELASEK§, KLAUS V. TOYKA§, ROLF DERMIETZEL¶, AND KLAUS WILLECKE*‖

*Institut für Genetik, Abteilüng Molekulargenetik, Universität Bonn, Römerstrasse 164, 53117 Bonn, Germany; ‡Institut für Biochemie, Universität Göttingen, Humboldtallee, 37073 Göttingen, Germany; §Neurologische Universitätsklinik, J.-Schneider-Strasse 11, 97080 Würzburg, Germany; and ¶Institut für Anatomie, Universität Regensburg, Universitätsstrasse 31, 93053 Regensburg, Germany

Communicated by Michael V. L. Bennett, Albert Einstein College of Medicine, Bronx, NY, June 12, 1996 (received for review February 15, 1996)

ABSTRACT **The gap junctional protein connexin32 is expressed in hepatocytes, exocrine pancreatic cells, Schwann cells, and other cell types. We have inactivated the connexin32 gene by homologous recombination in the mouse genome and have generated homozygous connexin32-deficient mice that were viable and fertile but weighed on the average ≈17% less than wild-type controls. Electrical stimulation of sympathetic nerves in connexin32-deficient liver triggered a 78% lower amount of glucose mobilization from glycogen stores, when compared with wild-type liver. Thus, connexin32-containing gap junctions are essential in mouse liver for maximal intercellular propagation of the noradrenaline signal from the periportal (upstream) area, where it is received from sympathetic nerve endings, to perivenous (downstream) hepatocytes. In connexin32-defective liver, the amount of connexin26 protein expressed was found to be lower than in wild-type liver, and the total area of gap junction plaques was ≈1000-fold smaller than in wild-type liver. In contrast to patients with connexin32 defects suffering from X chromosome-linked Charcot–Marie–Tooth disease (CMTX) due to demyelination in Schwann cells of peripheral nerves, connexin32-deficient mice did not show neurological abnormalities when analyzed at 3 months of age. It is possible, however, that they may develop neurodegenerative symptoms at older age.**

Gap junctions consist of intercellular channels, which are comprised of connexin proteins coded for by a multigene family of at least 12 members in mammals (1–3). Whereas gap junctions in excitable cells such as cardiomyocytes function in intercellular propagation of action potentials, their role in nonexcitable cells is less well understood. Among the hypothetical functions are growth control, metabolic coupling (i.e., exchange of nutrients), and coordination of metabolic activities (1–4). The latter function in parenchymal tissues is thought to regulate secretion of digestive enzymes in pancreas (5) and release of glucose from glycogen stores in liver (4, 6–8).

Hepatic gap junctions consist of large aggregates (plaques) of connexin channels. Connexin32 (Cx32) and connexin26 (Cx26) proteins are located in the same hepatic plaque (9). They can form heterotypic channels (10, 11), comprised of different but homogeneous hemichannels, and presumably also heteromeric channels (12), whose hemichannels are built up of different connexin types.

Recently, the connexin43 (Cx43) gene has been inactivated by homologous recombination in mice (13). The mutated homozygous animals died soon after birth with failure of pulmonary gas exchange due to malformations in the heart, where Cx43 was abundantly expressed in wild-type animals. It is not known how Cx43 gap junctions can influence heart development.

In humans, mutations in the Cx32 gene result in the X chromosome-linked Charcot–Marie–Tooth disease (CMTX; refs. 14–16), a neurodegenerative myelination disorder of the peripheral nervous system that is characterized by abnormally low nerve conduction. Cx32 is expressed in Schwann cells of peripheral nerves near the nodes of Ranvier and in Schmidt–Lanterman incisures, where it forms reflexive gap junctions that are thought to mediate signal propagation between the perinuclear and the periaxonal part of the same Schwann cell (14).

To study the function of Cx32 channels in murine cell types, such as hepatocytes, exocrine pancreatic cells, Schwann cells, and oligodendrocytes, we have generated homozygous and hemizygous Cx32 deficient mice by gene targeting. Here we report that Cx32-deficient mice exhibit defective propagation of signals received from sympathetic nerves in liver but do not show altered morphology and conduction of sciatic and facial nerve when analyzed at 3 months of age.

MATERIALS AND METHODS

Targeting Strategy. Sequences of Cx32 were subcloned from a recombinant phage obtained by screening of a BALB/c mouse library (17). Inactivation of Cx32 gene was achieved by the following strategy. The promoter less *neo*^{r} cassette (2.1-kb *Bgl*II/*Kpn*I fragment of pcDNA I NEO; Invitrogen) was inserted in frame into an *Eae*l site in exon 2 of the mouse Cx32 gene (17), resulting in a stop codon 90 nt after the translational start and a new start codon 15 bp further downstream. Insertion of a mutated polyoma enhancer element (Py, 181-bp EcoRI fragment of pMC1neo; ref. 18) in the 3′-untranslated region of the *neo*^{r} gene was carried out to enhance expression of the *neo*^{r} gene by the Cx32 promoter. The resulting targeting vector contained 3.1 kb of 5′-flanking DNA and 0.65 kb of 3′-flanking DNA of the Cx32 gene (Fig. 1*A1*).

Generation of Cx32-Deficient Mice. The targeting construct was linearized with *Sac*II and electroporated into 129SV J1 embryonic stem cells (19). G418-resistant clones were tested for homologous recombination into the Cx32 locus by PCR using primers derived from the *neo*^{r} gene (5′-TCTTACTC-CACACAGGCATAGAGTGTCTGC-3′) and the Cx32 gene (ref. 17; 5′-TCATTCTGCTTGTATTCAGGTGAGAG-GCGG-3′). Candidate clones for the expected targeting event were further analyzed by Southern blot hybridization of *Eco*RI- or *Pst*I- digested DNA, respectively, using the external,

The publication costs of this article were defrayed in part by page charge payment. This article must therefore be hereby marked "*advertisement*" in accordance with 18 U.S.C. §1734 solely to indicate this fact.

Abbreviations: Cx, connexin; CMTX, X chromosome-linked Charcot–Marie–Tooth disease.

†E.N. and C.B. contributed equally to this work.

‖To whom reprint requests should be addressed. e-mail: genetik@uni-bonn.de.

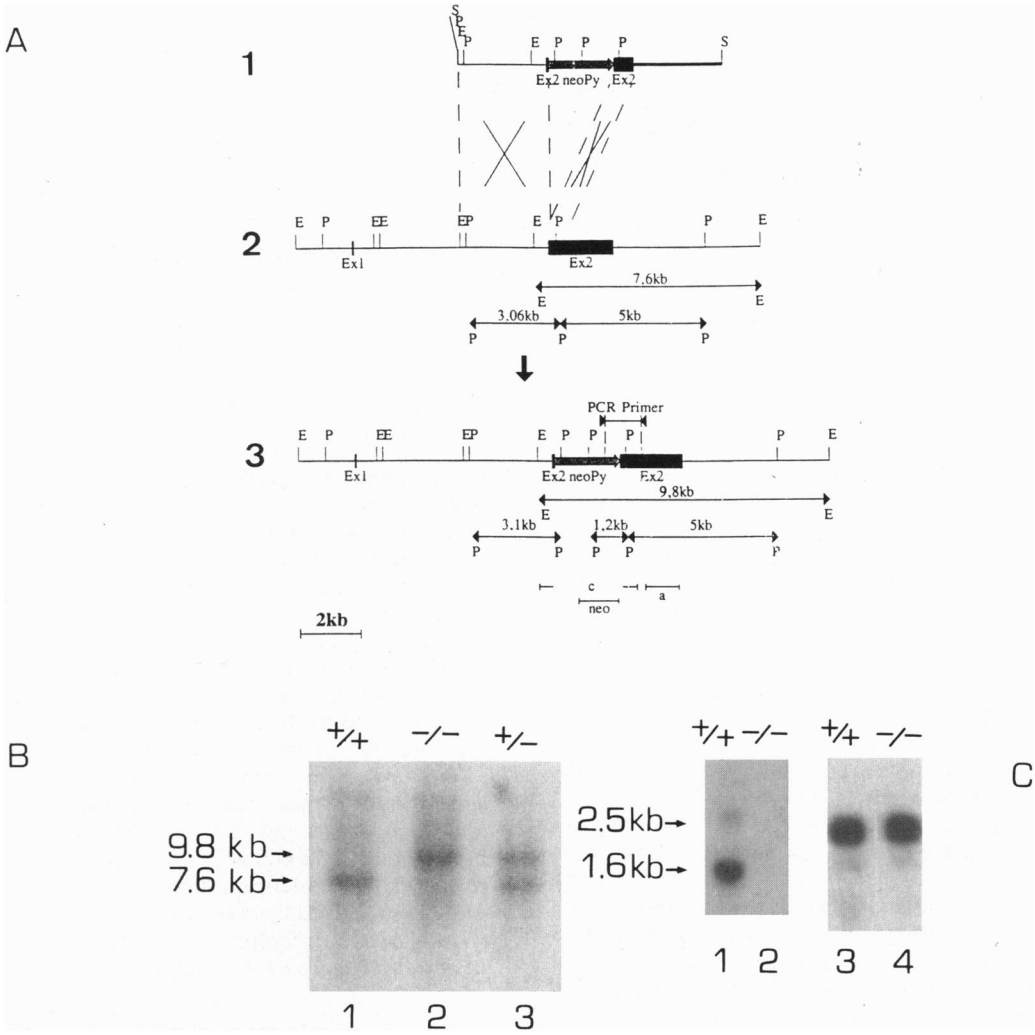

FIG. 1. Targeted disruption of the Cx32 gene and transcriptional analysis. (*A*) Targeting strategy. (*A1*) Targeting vector. Restriction sites are labeled as follows: S, *Sac*II; P, *Pst*I; and E, *Eco*RI. The DNA shown downstream of exon 2 (Ex2) was derived from pBluescript SK$^+$. (*A2*) Mouse Cx32 gene with the noncoding exon 1 (Ex1) and Ex2 harboring the complete reading frame. (*A3*) Recombinant locus and informative restriction fragments to be compared with the corresponding fragments in *A2*. The location of the 3′-external probe a, the internal probe c, the *neo* probe, and the positions of the primers for PCR are shown. (*B*) Southern blot hybridization using *Eco*RI-digested DNA from mouse tail biopsies (21) and the external 3′ probe. Lane 1, wild-type; lane 2, homozygous Cx32-deficient; lane 3, heterozygous Cx32-deficient. The 9.8-kb *Eco*RI fragment indicates the Cx32-defective allele. (*C*) Northern blot hybridization using 20 μg of total liver RNA and the Cx32 DNA probe (lanes 1 and 2) or the Cx26 DNA probe (lanes 3 and 4). +/+, Wild type; −/−, homozygous Cx32-deficient. Rehybridization of the Northern blot filters to a cytochrome *c* oxidase cDNA probe confirmed that similar amounts of RNA were loaded (data not shown).

internal, and neo-containing probes indicated in Fig. 1*A3*. Three clones (out of 165 *neo*^{r} clones), showing the correct homologous recombination event without additional integration of the construct, were isolated and injected into C57BL/6 blastocysts as described (20). Chimeric mice were crossed to C57BL/6 mice, and female agouti pups were genotyped (21) for transmission of the X chromosome-linked mutant Cx32 allele, which was achieved with one of the tested embryonic stem cell clones. Animal experiments were carried out in accordance with state law.

Northern Blot Analysis. Total cellular RNA, isolated as described (22), was electrophoretically separated on denaturating agarose gels and transferred to nylon membranes (Amersham). Blots were hybridized to a Cx26 probe (1.1-kb DNA fragment from the *Hin*dIII site of mouse Cx26 exon 2 to the 3′-end; ref. 17) or a Cx32 probe (*Sac*I/*Sma*I fragment representing the first 500 bp near the 5′-end of Cx32 exon 2 DNA (cf. Fig. 1*B*; ref. 17).

Protein Isolation and Immunoblot Analysis. Plasma membrane proteins were enriched by an alkali procedure (23) and subjected to standard immunoblot analysis using mixed polyclonal rabbit antibodies to mouse Cx32 (36) and Cx26 (24) or polyclonal rabbit antibodies to Cx43 (25), followed by incubation with [^{125}I]protein A and autoradiography for detection of the immunocomplexes.

Histology and Immunofluorescence. Sections (6 μm) of liver were cut on a cryostat and fixed in absolute ethanol (−20°C), whereas sciatic nerve fibers were teased and fixed in 2% paraformaldehyde. Immunofluorescence analysis was performed according to standard protocols (24). Rabbit polyclonal antibodies to mouse Cx32 and Cx26 were diluted 1:40. Fluorescein isothiocanate (FITC)-conjugated goat anti-rabbit IgG (Sigma) was diluted 1:50. Samples were mounted onto glass slides with *p*-phenylendiamine-glycerol mounting medium (Sigma).

Freeze-Fracture Electron Microscopy. Freeze-fracture analysis was performed after fixation of liver tissue with 2.5% glutaraldehyde, as described (26).

Perfusion of Mouse Livers and Neurostimulation. Mice were killed between 6 and 8 a.m., and livers from seven males from both wild-type and Cx32-deficient groups, were perfused via the portal vein with Krebs Henseleit bicarbonate buffer

containing 5 mM glucose, 2 mM lactate, and 0.2 mM pyruvate (7). Perivascular nerves were stimulated with rectangular monophasic impulses of 20 V and 2 ms duration at a frequency of 20 Hz for a period of 2 min. Noradrenaline (1 μM) or glucagon (1 nM) were infused for 2 min. Substrate balance was measured by enzymatic methods, and the rate of perfusion flow was determined by quantitating the effluate as reported (7).

Quantitative Enzymatic Degradation of Liver Glycogen. Livers were prepared and homogenized according to ref. 27. Glycogen was enzymatically degraded to glucose by incubation with amyloglucosidase and quantitated using standardized reagents (Sigma kit no. 115; cf. ref. 28). From each value obtained, the level of free glucose in liver was subtracted. The livers were taken from male mice at 10 weeks of age.

Electrophysiological Measurements. Motor and mixed afferent nerve conduction were measured as described (29) in the sciatic and facial nerves of mice.

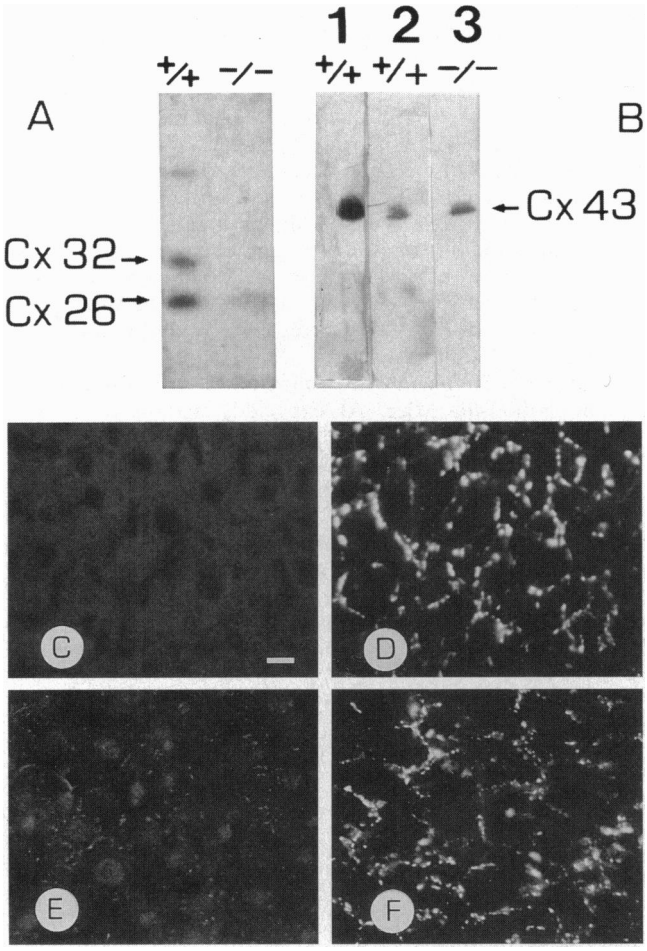

FIG. 2. Immunochemical analyses of connexin proteins expressed in liver. (*A*) Immunoblot of mouse liver protein (23) using a mixture of specific Cx32 and Cx26 antibodies for analysis (24). Cx32 and Cx26 protein were detected in wild-type liver (+/+), whereas the Cx32 protein was absent and the amount of the Cx26 protein was decreased in Cx32-deficient liver (−/−). (*B*) Immunoblot of protein extracts (23) using specific Cx43 antibodies (25) for analysis. Lane 1, adult mouse heart (+/+; control); lane 2, Cx32 wild-type (+/+) mouse liver; and lane 3, Cx32-deficient (−/−) mouse liver. (*C–F*) Indirect immunofluorescence analysis (24) of liver sections. (*C* and *E*) Cx32 (−/−) mice. (*D* and *F*) Cx32 (+/+) mice. Antibodies specific to Cx32 (*C* and *D*) or to Cx26 protein (*E* and *F*) were used. Note that no Cx32 protein was detected in Cx32-deficient liver, in which weak immunofluorescence of Cx26 protein was found. Wild-type mouse liver does not show the increased concentration of Cx26 in periportal fields as previously noticed in rat liver (9). Morphology of liver sections was monitored by phase contrast microscopy. (*C–F*, bar = 11.5 μm.)

RESULTS

Genotype and Gross Phenotype of Cx32-Deficient Mice. To inactivate the Cx32 gene in mice, we used a targeting vector where a *neo*^{r} gene cassette was inserted into exon 2 of the Cx32 gene, 30 codons after the translational start site (Fig. 1*A*). Using an external probe a (cf. Fig. 1*A3*), we showed by Southern blot hybridization (Fig. 1*B*) that only the informative *Eco*RI fragment of 9.8 kb could be detected in genomic DNA from homozygous Cx32-deficient animals. The correct gene targeting was confirmed by use of the internal probe c and one specific for detection of the *neo* gene (indicated in Fig. 1*A3*; results not shown). Furthermore, as expected, no Cx32 transcript was detected after Northern blot hybridization in total RNA from Cx32 (−/−) liver, in contrast to Cx32 (+/+) control liver (Fig. 1*C*, lanes 1 and 2). The amounts of Cx26 mRNA were similar in Cx32-defective and wild-type liver (Fig. 1*C*, lanes 3 and 4).

Fertility and gross morphology of the Cx32-deficient mice were normal, with the exception that the average weight was ≈17% less, compared with wild-type animals of the same genetic background (i.e., F1 hybrids of C57BL/6 and 129SV mice). This was independent of age (7–28 weeks) and gender (86 males and 130 females were investigated).

Cx32-Deficient Liver Contained Less Cx26 Protein and Much Smaller Gap Junction Plaques Than Wild-Type Liver. As expected, no Cx32 protein was found in Cx32 defective livers (Fig. 2*A*) but, surprisingly, the amount of Cx26 protein in Cx32 (−/−) livers was considerably lower than in wild-type livers (Fig. 2*A*). This was confirmed by immunofluorescence analysis, which showed no signals with anti-Cx32 in Cx32 (−/−) liver (Fig. 2*C*), but less intensive and fewer punctate signals with anti-Cx26 in Cx32-defective livers (Fig. 2*E*) than in wild-type controls (Fig. 2 *D* and *F*, respectively). Cx32-defective livers contained about the same low amount of Cx43 protein as wild-type livers (Fig. 2*B*). The amount of Cx43

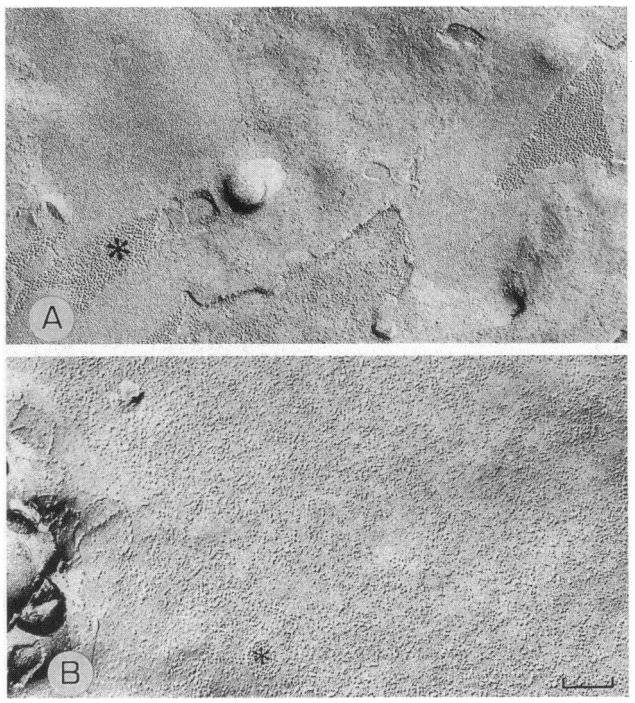

FIG. 3. Freeze-fracture electron micrographs of Cx32 (+/+) (*A*) and Cx32 (−/−) (*B*) mouse liver. Apical portions of lateral plasma membranes below the area of tight junctions are shown. Gap junction plaques are indicated by asterisks. The total number of intramembranous particles in Cx32 (+/+) versus Cx32(−/−) liver was not increased. *A* shows preferably an E-face, which normally has fewer particles than the P-face (shown in *B*). (Bar = 3.5 μm.)

protein, which is not coexpressed with Cx32 protein in hepatocytes, but is expressed in other cell types of liver (4), was about the same in Cx32-defective livers and in wild-type livers (Fig. 2*B*).

Areas of contact membranes in Cx32 (+/+) liver (227 μm^2) and Cx32 (−/−) liver (2235 μm^2) were morphometrically analyzed on freeze-fracture electron micrographs. Examples are shown in Fig. 3 *A* and *B*, respectively. The freeze-fracture replicas were collected randomly. Since mice, in contrast to rats, show no gradient of Cx32 and Cx26 expression in liver lobules, the samples were considered to give a statistically reliable image of gap junction distribution. It was found that the total area of gap junctional plaques in Cx32-deficient liver (0.16 μm^2) was ≈1000-fold smaller, compared with wild-type liver.

Only Low Amounts of Glucose Were Mobilized by Electrical Stimulation of Sympathetic Nerves in Cx32-Deficient Mice. To test whether metabolic cooperativity among hepatocytes was impaired by disruption of the Cx32 gene, we stimulated the sympathetic plexus, which is located as ramification around the portal vein in the liver hilus. After electrical nerve stimulation of perfused Cx32-deficient liver (7), the amount of glucose released was decreased by 78% when compared with wild-type livers (Fig. 4 *A* and *B*). In contrast, glucose release after infusion of noradrenaline or glucagon was about the same in Cx32-deficient and control livers (Fig. 4 *A* and *B*), suggesting that circulating noradrenaline or glucagon molecules acted via their receptors on all or almost all cells, without signal propagation via gap junctions. The hepatic flow (7) was slightly higher in Cx32-deficient than in wild-type liver (Fig. 4*A*); this was of no functional significance, since the glucose balance related to grams of tissue was calculated considering the flow (glucose balance in μmol/min/g equals the concentration difference between outflow and inflow in μmol/ml multiplied by flow in ml/min/g).

The Maximal Accumulation of Glycogen in Cx32-Deficient Liver Was Higher Than in Wild-Type Liver. We found that the maximal amount of glycogen accumulated during the diurnal rhythm (between midnight and 8 a.m.) in the livers of Cx32-deficient mice (−/Y) was ≈10% higher than in wild-type livers (+/Y). Since the rate of glycogen degradation was similar, the minimal amount of glycogen in Cx32-deficient liver was reached later, between 4 and 6 p.m. instead of between 2 and 4 p.m., measured in wild-type liver (Fig. 5; light phase in the mouse room, 4 a.m. to 4 p.m.).

Young Cx32-Deficient Mice Showed Similar Nerve Conduction as Wild-Type Mice. As expected, analysis of indirect immunofluorescence revealed no immunoreactivity with anti-Cx32 in sciatic nerves of Cx32-deficient mice, although specific immunoreactivity could easily be detected in wild-type nerves (Fig. 6 *B* and *A*, respectively). Next, we analyzed motor and mixed afferent nerve conduction in the sciatic nerve, as well as refractory periods and motor nerve conduction in the facial nerve. We found that all these parameters were normal in 5 female Cx32 (+/−) mice, 4 female Cx32 (−/−) mice, and 10 male Cx32 (−/Y) mice when compared with 16 age-matched

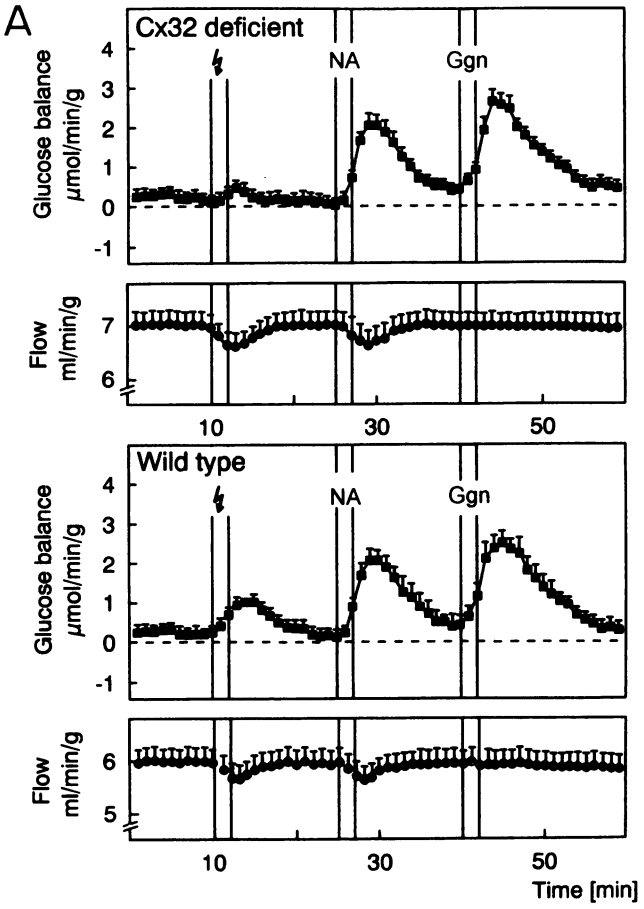

B

Glucose output (μmol · g liver^{-1})

	↯	NA	Ggn
Wild type	6.4± 0.6	13.2±1.3	17.8±1.7
Cx32 deficient	1.4±0.2*	12.9±0.7	17.0±0.9

FIG. 4. Kinetics of hepatic glucose release from perfused mouse liver by electrical stimulation (↓) of hepatic sympathetic nerve bundles, compared with stimulation with noradrenaline (NA) and glucagon (Ggn). (*A*) Cx32-deficient liver (males −/Y, n = 7) and Cx32 wild-type liver (males +/Y, n = 7). The upper curve of each represents the kinetics of glucose release; the lower curve of each represents the portal flow rate. (*B*) The numerical results of glucose mobilization are summarized in this table. Data represent the areas under the appropriate peaks in *A* ± SEM. Student's t test for unpaired values of Cx32-deficient versus control animals yielded P = 0.0005.

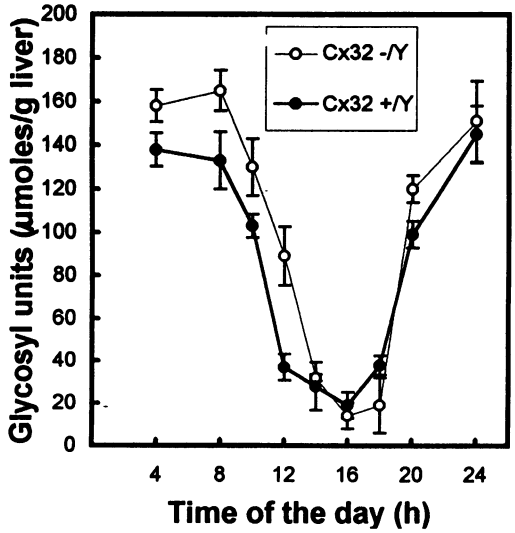

FIG. 5. Diurnal rhythm of glycogen content in livers of Cx32 (−/Y) mice (○) and Cx32 (+/Y) wild-type mice (●). Glycogen was quantitated enzymatically (27, 28). Each point represents averaged results ± SEM, based on measurements with four livers, except at midnight and 4 a.m., when two livers each were used. Light interval in the mouse room was from 4 a.m. to 4 p.m.

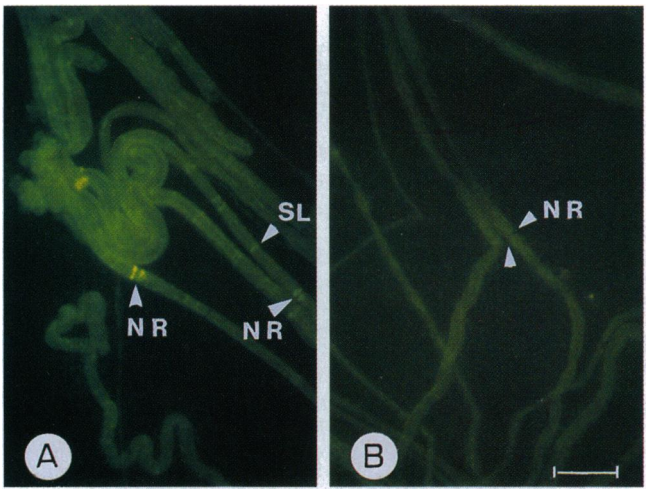

FIG. 6. Immunofluorescence analysis with anti-Cx32 (24) of teased sciatic nerve fibers. *A* [from Cx32 (+/+) mouse] shows consistent labeling at the nodes of Ranvier (NR) and Schmidt–Lanterman incisures (SL), while *B* [from Cx32 (−/−) mouse] is devoid of immunolabel. A node of Ranvier in *B* is indicated by arrowheads. Presence of nodes of Ranvier was assessed by phase contrast microscopy. (*A* and *B*, bar = 17 μm.)

control mice (2–4.5 months old). These results are listed in Table 1. No definitive morphological abnormality of the myelin sheath was noticed by electron microscopy on cross sections of sciatic nerve in 3-month-old animals (data not shown).

DISCUSSION

Our results strongly support the hypothesis that gap junctions in murine liver mediate intercellular parenchymal propagation of signals received by a subset of hepatocytes from sympathetic nerve endings, presumably through the release of noradrenaline via α1-receptors (8). It had been found before in perfused rat liver that activation of sympathetic liver nerves stimulated glucose release, among other alterations of liver metabolism, and decreased the hepatic flow rate (cf. 8). Synaptically released noradrenaline can bind to receptors on hepatocytes and lead to an intracellular increase of inositol 1,4,5-trisphosphate, which can release calcium from intracellular pools. Both of these second messenger molecules have been shown to diffuse through gap junctions in cultured hepatocytes (30). Murine liver (31), in contrast to human liver (32, 33), is only sparsely innervated. The endings of murine sympathetic liver nerves have been mainly detected near periportal hepatocytes (31) and nearby nonparenchymal liver cells (cf. ref. 8). Cx32 is expressed in hepatocytes but not in nonparenchymal cells (4). Thus, the genetic defect in Cx32-deficient mouse liver should primarily influence intercellular communication among hepatocytes. Our data are consistent with this conclusion. We found that glucose release was affected in Cx32-deficient liver but not the portal flow rate, which is controlled by nonparenchymal cells (cf. Fig. 4). These cells presumably express Cx43 protein, whose total amount appears to be the same in Cx32 (−/−) and Cx32 (+/+) liver (cf. Fig. 2*B*).

In contrast, the amount of Cx26 protein in Cx32 (−/−) liver was significantly lower than in control liver (Fig. 2*A*), although the amount of Cx26 mRNA appears to be the same (Fig. 1*C*). Both proteins had been shown to be localized in the same hepatic gap junctional plaque (9). Our results suggested that Cx32 protein stabilized the amount of Cx26 protein in murine liver. Whether this occurred by interaction in heterotypic (10, 11) or heteromeric (12) gap junction channels remains to be investigated. Our results demonstrated that the total area of gap junction plaques in Cx32 (−/−) liver was ≈1000-fold smaller than in control liver (cf. Fig. 3). Future experiments will have to show to what extent electrical and dye coupling is altered in slices from Cx32-deficient versus wild-type liver.

Interestingly, we found a 10% higher accumulation of glycogen in Cx32 (−/Y) livers during the early morning hours of the diurnal cycle, compared with control livers (Fig. 5). Since the degradation of glycogen was similar, the minimal amount was reached 2 h later in Cx32 (−/Y) liver than in wild-type liver. Currently we are investigating how the Cx32 defect and the difference in glycogen accumulation during the diurnal cycle are related.

In humans, mutations in the Cx32 gene have been reported to cause CMTX (14–16). This peripheral neuropathy is characterized by slowly progressive weakness of distal muscles, which is associated with decreased nerve conduction and demyelination of peripheral nerves. The symptoms become apparent during the second decade of life. In the expression system of paired *Xenopus* oocytes, it has been found that several of the human Cx32 mutations lead to defective Cx32 protein, which can affect the function of Cx26 channels in a transdominant negative manner (34). Some of the nonsense CMTX mutations are expected not to express functional Cx32 protein (14). In contrast, Cx32 (−/−) mice that do not appear to express any Cx32 protein (cf. Fig. 2 *A* and *C*).

So far, no dysfunction of liver has been reported for CMTX patients. This difference in the Cx32 (−/−) mice, described here, can be explained by previous findings that human liver (32, 33) is much more densely innervated than mouse liver (31). Thus, the absence of Cx32-containing gap junctions in the liver of CMTX patients may affect glucose mobilization, triggered by sympathetic nerve signaling, to a lesser extent than in Cx32 (−/−) or (−/Y) mouse liver. Our results that no abnormalities of sciatic nerves were noticed in 3-month-old Cx32 (−/−) mice could mean that another unidentified connexin may compensate for the missing Cx32 protein in mouse Schwann cells (35). Alternatively, the particular morphology of motoneurons with long neurites, which are primarily affected by CMTX, may have more severe influence in man than in mice. Furthermore, the Cx32-deficient mice may

Table 1. Nerve conduction studies in wild-type and Cx32-deficient mice

Group	Wild-type mice			Cx32 (−/Y)	Cx32 (−/−)	Cx32 (+/−)
	Female	Male	Female and male			
No. of animals	3	13	16	10	4	5
Sciatic nerve						
Motor nerve conduction velocity, m/s	30 ± 8	35 ± 9*	34 ± 9†	36 ± 10	41 ± 6	37 ± 6
Mixed afferent nerve conduction velocity, m/s	43 ± 9	47 ± 15	46 ± 14	42 ± 14	54 ± 10	54 ± 14
Facial nerve						
Absolute refractory time, ms	0.6 ± 0.2	0.6 ± 0.3	0.6 ± 0.2	0.5 ± 0.2	0.6 ± 0.0	0.6 ± 0.1

Data are given as means ± SD.
*n = 11.
†n = 14.

develop degeneration of peripheral nerves at older age. Recently it was found that 12-month-old, Cx32-deficient mice showed subtle electrophysiological abnormalities and pathological alterations of myelin degeneration in peripheral nerves (P. Anzini, R. Martini, J.Z., and K.V.T., unpublished data).

Our finding that gap junctions in murine liver mediate intercellular propagation of signals received from sympathetic nerves may be valid for other tissues as well, such as vascular smooth muscle cells or cardiomyocytes, which are also connected by connexin channels. The Cx32-deficient mice described in this study should be very useful to investigate the effects of lacking Cx32 channels on the physiology of other cell types, such as Schwann cells, oligodendrocytes, and exocrine pancreatic cells. Furthermore, the possible involvement of Cx32 channels in tumorigenesis can be studied with these mice.

We thank U. Ebertshäuser for technical assistance, Drs. R. Jaenisch and R. Fässler for the J1 embryonic stem cell line, and Drs. A. Gossler and R. Korn for technical advice concerning embryo manipulations. This work was supported by grants from the Deutsche Forschungsgemeinschaft to F.S. and K.J. (SFB 402), K.V.T. and R.D. (SFB 43,C7), and K.W. (SFB 284, C1), the Dr. Mildred Scheel Stiftung für Krebsforschung, and the Fonds der Chemischen Industrie to K.W.

1. Beyer, E. C. (1993) *Int. Rev. Cytol.* **137C,** 1–37.
2. Bennett, M. V. L., Barrio, L. C., Bargiello, T. A., Spray, D. C., Hertzberg, E. L. & Saez, J. C. (1991) *Neuron* **6,** 305–320.
3. Paul, D. L. (1995) *Curr. Opin. Cell Biol.* **7,** 665–672.
4. Spray, D. C., Saez, J. C., Hertzberg, E. L. & Dermietzel, R. (1994) in *The Liver: Biology and Pathology*, eds. Arias, I. M., Boyer, J. L., Fausto, N., Jacoby, D. W. & Schachter, D. (Raven, New York), pp. 951–968.
5. Meda, P., Vozzi, C., Ullrichs, S., Dupont, E., Charrolais, Sutter, E. & Bosco, D. (1995) *Prog. Cell Res.* **4,** 281–287.
6. Iwai, M., Mishashita, T. & Shimazu, T. (1991) *Eur. J. Biochem.* **200,** 69–74.
7. Seseke, F., Gardemann, A. & Jungermann, K. (1992) *FEBS Lett.* **301,** 265–270.
8. Gardemann, A., Püschel, G. O. & Jungermann, K. (1992) *Eur. J. Biochem.* **207,** 399–411.
9. Nicholson, B. J., Dermietzel, R., Teplow, D., Traub, O., Willecke, K. & Revel, J.-P. (1987) *Nature (London)* **329,** 732–734.
10. Barrio, L. C., Suchyna, T., Bargiello, T., Xu, L. X., Roginsky, R. S., Bennett, M. V. L. & Nicholson, B. J. (1991) *Proc. Natl. Acad. Sci. USA* **88,** 8410–8414.
11. Elfgang, C., Eckert, R., Lichtenberg-Fraté, H., Butterweck, A., Traub, O., Klein, R. A., Hülser, D. F. & Willecke, K. (1995) *J. Cell Biol.* **129,** 805–817.
12. Stauffer, K. A. (1995) *J. Biol. Chem.* **270,** 6768–6772.
13. Reaume, A. G., de Sousa, P. A., Kulharni, S., Langielle, B. L., Zhu, D., Davies, T. C., Juneja, S. C., Kidder, G. M. & Rossant, J. (1995) *Science* **267,** 1831–1834.
14. Bergoffen, J., Scherer, S. S., Wang, S., Scott, M. D., Bone, L. J., Paul, D. L., Chen, K., Lensch, M. W., Chance, P. F. & Fischbeck, K. H. (1993) *Science* **262,** 2039–2042.
15. Fairweather, N., Bell, C., Cochrane, S., Chelly, J., Wang, S., Mostacciaolo, M. L., Monaco, A. P. & Haites, N. E. (1994) *Hum. Mol. Genet.* **3,** 29–34.
16. Ionasescu, C. V., Searby, C. & Ionasescu, R. (1994) *Hum. Mol. Genet.* **3,** 355–358.
17. Hennemann, H., Kozjek, G., Dahl, E, Nicholson, B. J. & Willecke, K. (1992) *Eur. J. Cell Biol.* **58,** 81–89.
18. Thomas, K. R. & Capecchi, M. R. (1987) *Cell* **51,** 503–512.
19. Li, E., Bestor, T. H. & Jaenisch, R. (1992) *Cell* **69,** 915–926.
20. Hogan, B., Beddington, R., Constantini, F. & Lacy, E. (1994) *Manipulating the Mouse Embryo* (Cold Spring Harbor Lab. Press, Plainview, NY), pp. 196–204.
21. Laird, P., Zijderveld, A., Linders, K., Rudnicki, M. A., Jaenisch, R. & Berns, A. (1991) *Nucleic Acids Res.* **19,** 4293.
22. Chomczynski, P. & Sacchi, N. (1987) *Anal. Biochem.* **162,** 156–159.
23. Hertzberg, E. L. (1984) *J. Biol. Chem.* **259,** 9936–9943.
24. Traub, O., Look, J., Dermietzel, R., Brümmer, F., Hülser, D. F. & Willecke, K. (1989) *J. Cell Biol.* **108,** 1039–1057.
25. Traub, O., Eckert, R., Lichtenberg-Fraté, H., Elfgang, C., Bastide, B., Scheidtmann, K. H., Hülser, D. & Willecke, K. (1994) *Eur. J. Cell Biol.* **64,** 101–112.
26. Dermietzel, R. (1974) *Cell Tissue Res.* **148,** 565–576.
27. Keppler, D. & Decker, K. (1969) *Eur. J. Biochem.* **10,** 219–225.
28. Carroll, J. J., Smith, N. & Babson, A. L. (1970) *Biochem. Med.* **4,** 171–176.
29. Montag, D., Giese, K. P., Bartsch, U., Martini, R., Lang, Y., Blütmann, H., Karthigasan, J., Kirschner, D. A., Wintergerst, E. S., Nave, K. A., Zielasek, J., Toyka, K. V., Lipp, H.-P. & Schachner, M. (1994) *Neuron* **13,** 229–246.
30. Saez, J. C., Connor, J. A., Spray, D. C. & Bennett, M. V. L. (1989) *Proc. Natl. Acad. Sci. USA* **86,** 2708–2712.
31. Yamada, E. (1965) *Okajimas Folia Anat. Jpn.* **40,** 663–677.
32. Forssmann, W. G. & Ito, S. J. (1977) *Cell Biol.* **74,** 299–313.
33. Sasse, D. (1986) in *Regulation of Hepatic Metabolism: Intra- and Intercellular Compartmentation*, eds. Thurman, G. R., Kauffman, F. C. & Jungermann, K. (Plenum, New York), pp. 3–25.
34. Bruzzone, R., White, T. W., Scherer, S. S., Fischbeck, K. H. & Paul, D. L. (1994) *Neuron* **13,** 1253–1260.
35. Chandross, K. J., Chanson, M., Spray, D. C. & Kessler, J. A. (1995) *J. Neurosci.* **15,** 262–273.
36. Traub, O., Look, J., Paul, D. & Willecke, K. (1987) *Eur. J. Cell Biol.* **43,** 48–54.